Acta Geochim (2025) 44:1040–1058
https://doi.org/10.1007/s11631-025-00764-z

REVIEW ARTICLE

# Distribution and human health risk assessment of cadmium, arsenic, mercury, lead, and iron in settling particles from the transboundary estuary in three rivers of Côte d'Ivoire, West Africa

**Dehoule N'Guessan Fulgence Kouassi[1] · Assy Eudes Yapi[1] · N'Guessan Louis Berenger Kouassi[2] · Koffi Marcellin Yao[3] · Aoua Sougo Coulibaly[1]**

Received: 2 August 2024 / Revised: 22 January 2025 / Accepted: 23 January 2025 / Published online: 15 February 2025


**Abstract** Pollution of transboundary rivers can result from anthropogenic activities in their watersheds. In this study, sediment traps were deployed to determine the fluxes, concentrations, and health risks associated with arsenic, cadmium, mercury, lead, and iron in the estuaries of three transboundary rivers (Comoé, Bia, and Tanoé) in West Africa. Thus, the analysis of metal-associated sedimentation particle samples collected in rainy, flood, and dry seasons was required. Sediment traps were used to calculate the metal fluxes associated with sedimentation particles towards the Atlantic Ocean. Finally, the carcinogenic and non-carcinogenic risks of ingestion and dermal contact associated with sedimentation particles were assessed. The results showed that the total concentrations of trace metals in particulate matter were higher than in the UCC (Upper Crust Continental), with the exception of lead. The highest fluxes of lead, mercury, iron and arsenic associated with sedimented particles were observed during flood periods in the estuary of the Comoé, Bia and Tanoé rivers. Cadmium fluxes associated with sedimentation particles were highest in the rainy season in the Bia and Comoé estuaries and in the flood season in the Tanoé estuary. Pearson's correlation analysis and the enrichment factor showed that the trace metals were derived from anthropogenic activities such as mining and farming. In addition, contamination indices showed that sediment particles in the estuaries of the three rivers were severely contaminated with mercury. However, the results of potential human health risks associated with trace metals show that there is no probability of exposure of the community to harmful and carcinogenic effects through ingestion and dermal absorption of sediment particles. It is essential to integrate the information from this study into policy- and decision-making processes for better management of transboundary river water resources in coastal countries, particularly the Côte d'Ivoire.

**Keywords** Trace metals · Settling particles · Transboundary rivers · Carcinogenic and non-carcinogenic risks · Estuary · West Africa

## 1 Introduction

River estuaries are corridors of exchange between continental rivers and marine environments. During these exchanges, numerous reactions take place (physical, chemical, biochemical, geochemical, biogeochemical, etc.) (Ghosh et al. 2016). This particularity makes an estuary a unique ecosystem rich in biodiversity and conducive to human activities. In recent decades, these environments have been heavily affected by anthropogenic activities such as mining, agriculture, and industry (Li et al. 2007; Zhao et al. 2015). These activities exert strong pressure on estuarine systems, leading to their pollution through various pollutants. In addition, those metals become even more dangerous in areas with high erosion and sediment flow (Panagos et al. 2021).

✉ Dehoule N'Guessan Fulgence Kouassi
fulgencedehoule@gmail.com

[1] Département de Géologie Marine et sédimentologie, UFR STRM, Université Félix Houphouët-Boigny, 22 BP 582, Abidjan 22, Côte d'Ivoire

[2] Département de Mathématiques, Physique et Chimie, UFR Sciences Biologiques, Université Peleforo GON COULIBALY, BP 1328, Korhogo, Côte d'Ivoire

[3] Centre de Recherches Océanologiques (CRO), 29 rue des Pêcheurs, BP V 18, Abidjan, Côte d'Ivoire

Among these pollutants, trace metals (TMEs) have become a global concern for the following reasons: their toxicity, their threat for food safety, their persistence in the environment, their bioaccumulation, their non-biodegradable nature, and their ability to accumulate (Xu et al. 2015; Bastami et al. 2015; Singh and Kumar 2017). However, environmental contamination by these metals needs to be monitored in a special way, as it can have consequences for humans. These negative consequences include skin, kidney and liver diseases, cancers, and so on. Due to their high absorption capacity, fine sediments (particles in sedimentation) will trap TMEs in aquatic environments (Hamzeh et al. 2014). Thus, the study of TMEs requires knowledge of sedimented particles, as they trace the history of aquatic ecosystems. To study the history of an ecosystem based on sedimentation particles, a tool has been developed for sampling these sedimentation particles. This tool is called a sediment trap. It is an efficient, passive collector and accumulator of sediment particles. Sediment traps can be used to calculate particulate matter fluxes in lacustrine, estuarine, and marine ecosystems (Helali et al. 2016). For the effectiveness of these sediment traps, it is recommended to use sediment traps with aspect ratios (height/diameter) > 5 (Botwe et al. 2017; de Vicente et al. 2010).

The Comoé, Bia, and Tanoé rivers in Côte d'Ivoire, West Africa, originate from countries such as Ghana and Burkina Faso. These rivers drain large flows of sedimented particles associated with metals from anthropogenic activities located in their watersheds (Kouassi et al. 2022). These anthropogenic activities are generally agriculture and artisanal gold mining. These flows of sedimented particles associated with metals are discharged into the Atlantic Ocean via the Ebrié and Aby lagoons, which teem with important aquatic resources needed by the surrounding populations (Kouassi et al. 2022). According to Ouattara et al. (2018), these surrounding populations, estimated at over 3 million people, use the water from these rivers for bathing and drinking without prior treatment. As a result, they can ingest sediment particles associated with the metals, which can lead to adverse effects such as skin and organ cancer from arsenic and cadmium. Also, fishing activities are practiced in the estuary rivers of Comoé, Bia, and Tanoé, and the fish products are consumed by 70% of the Côte d'Ivoire population (Kouassi et al. 2022). These rivers are impacted by mining activities which are an important source of mercury in the environment (Aldous et al. 2024). It has been reported that people living around the Minamata Bay in Japan have been poisoned after consumption of mercury-contaminated fish (Ekino et al. 2007). Therefore, the population in Côte d'Ivoire may be exposed to deleterious effects through the consumption of fish from the Comoé, Bia, and Tanoé rivers.

The general objective of this study was to examine the concentrations of arsenic, cadmium, lead, mercury, and iron in sedimentation particles in the estuary of the Comoé, Bia, and Tanoé rivers. This is necessary in order to understand the influence of human activities on the level of pollution of sedimentation particles and the potential health risks for populations. To this end, we analyzed metal-associated sedimentation particle samples collected from May 2019 to February 2020, covering the rainy, flood, and dry seasons. The carcinogenic and non-carcinogenic risks associated with ingestion and dermal contact of metal-associated sedimentation particles were assessed. Finally, the fluxes of metal-related sedimentation particles into the Atlantic Ocean were also calculated.

## 2 Materials and methods

### 2.1 Study area

The study area covers the Comoé, Bia, and Tanoé estuaries (Fig. 1). The estuaries of these three rivers form part of a fluvial-lagoon environment between the Comoé, Bia, and Tanoé rivers and the Ebrié and Aby lagoons, respectively. Average flows are 65 $m^3$/s for the Bia, 142 $m^3$/s for the Tanoé, and 106 $m^3$/s for the Comoé.

The climate in the study area is humid equatorial, with two rainy and two dry seasons. The first rainy season runs from mid-May to the end of July, while the second begins in early October and ends in mid-December, while the first dry season runs from mid-December to mid-March, and the second from mid-July to the end of September. Rainfall is high during flood periods, ranging from 1400 to 2000 mm/year from north to south. Temperatures range from 25 to 32 °C.

This study area was chosen because of its high anthropogenic activity, high population density, and commercial crops. The main anthropogenic activity is gold mining, which takes place upstream, and the main economic activities are agriculture and fishing (Kouassi et al. 2022).

Soils in these watersheds are used for residential, agricultural, industrial, and semi-industrial purposes. Agricultural, domestic, and industrial effluents, as well as wastewater from industrial and other upstream communes (Bonoua, Yaou, Aboisso), can find their way into the downstream waters of the Comoé, Bia, and Tanoé rivers via surface runoff and drains. Soil erosion is a major global environmental problem that has caused numerous problems involving soil degradation, sedimentation of watercourses, ecological degradation, and diffuse pollution. In the study area, an investigation of the dynamics of land use in the estuary of the Comoé, Bia, and Tanoé rivers revealed a regression in vegetation cover in favor of mosaics of crops, fallow land, and built-up areas. The development of cultivated areas and built-up areas destabilizes the soil structure and encourages erosion. This degradation of the plant cover encourages the

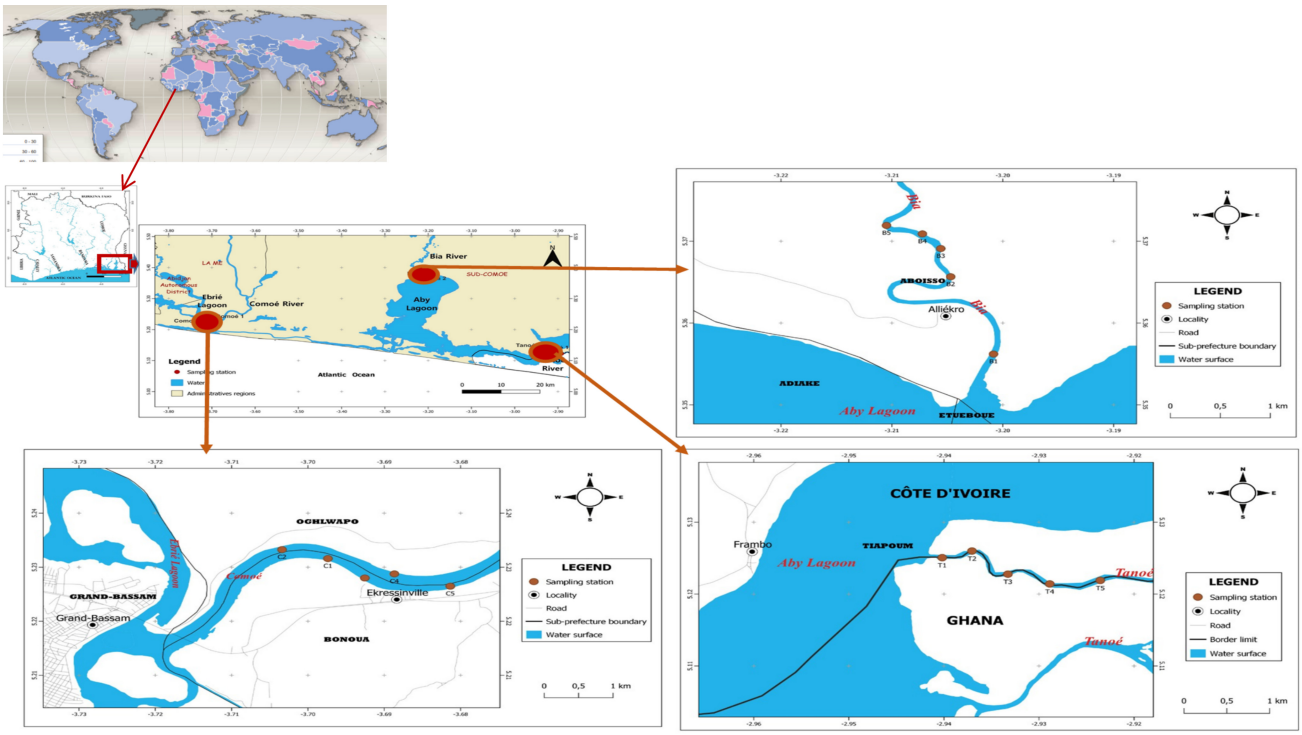


**Fig. 1** Study area and sampling stations

transport of sediment and an increase in suspended solids in the Aby lagoon (Gauze et al. 2019). It also increases the flow of suspended particles towards the Atlantic Ocean via the Aby and Ebrié lagoons.

## 2.2 Sampling

A total of 45 samples of sedimented particles were collected from the estuary of the Comoé (C), Bia (B), and Tanoé (T) rivers (Fig. 1). The labeled samples and the longitude and latitude values of the sampling points are shown in Table 1. Sedimentation particles were collected using sediment traps, which were cylindrical sediment traps made of polyvinyl chloride (PVC) with aspect ratios of 6.0. The sediment traps were deployed at five stations (1, 2, 3, 4, and 5) in the estuary of the Comoé, Bia, and Tanoé rivers, where water depths vary from 9 to 11 m, to collect settling particles. They were positioned at a water depth of 1.8 m from the seabed, and carefully capped prior to recovery every 2 months over a 9-month period (May 2019 to February 2020), to keep the trapped material intact (Botwe et al. 2017). After recovery, the contents of the sediment traps were carefully collected and then placed in polyethylene zipper bags, which were carefully sealed, labeled, and placed in a cooler where the temperature was maintained at 4 °C using ice packs. In the laboratory, the trapped sediments were placed in high-density polyethylene bottles for subsequent freeze-drying.

**Table 1** Characteristics of the sampling stations

| River | Locality name | Sample ID | Longitude (W) | Latitude (N) |
|---|---|---|---|---|
| Comoé | Adjekro 1 | C1 | − 3.700611 | 5.234869 |
| | Adjekro 2 | C2 | − 3.705308 | 5.240322 |
| | Fishermen's camp | C3 | − 3.688933 | 5.231669 |
| | Moosou 1 | C4 | − 3.687367 | 5.233886 |
| | Moosou 2 | C5 | − 3.676203 | 5.243308 |
| Bia | Bianouan 2 | B1 | − 3.202208 | 5.356886 |
| | Mixed area | B2 | − 3.200406 | 5.365589 |
| | Cacao culture | B3 | − 3.202742 | 5.369492 |
| | Mixed area | B4 | − 3.205519 | 5.371356 |
| | Bianouan 2 | B5 | − 3.214408 | 5.370594 |
| Tanoé | Mixed area | T1 | − 2.942781 | 5.131156 |
| | Mixed area | T2 | − 2.940236 | 5.127781 |
| | Mixed area | T3 | − 2.924842 | 5.126428 |
| | Mixed area | T4 | − 2.929308 | 5.124831 |
| | Entrance to camp | T5 | − 2.933725 | 5.124969 |

## 2.3 Pre-treatment and chemical analysis

Samples of 0.1 g of homogenized dry sedimentation particles were placed in Teflon tubes, which were washed with dilute nitric acid. The samples underwent hot mineralization,

using aqua regia made up of 3 mL hydrochloric acid and 1 mL nitric acid. The samples were heated to 120 °C for 3 h. After cooling in ambient air, the final volume was reduced to 50 mL and left to stand overnight (Loring and Rantala 1992). Metals were determined by Varian AA 20 atomic absorption spectrometry (AAS). Iron was analyzed using the flame technique, As, Cd, and Pb by the graphite furnace technique, and Hg by the cold vapor technique. The detection limits for the metals analyzed were: 0.03 mg/kg for As; 0.051 mg/kg for Hg; 0.002 mg/kg for Cd; 0.006 mg/kg for Pb and Fe (Ouattara et al. 2018).

### 2.4 Quality control

Prior to metal analysis, automatic calibration of the AAS was performed by aspirating a bulk standard (multi-element standard solution for ICP; Fluka Analytical, Switzerland). Procedural blanks and a certified reference material for settling particles were treated in the same way as the field samples and analyzed in duplicate, while reference materials were analyzed in triplicate. Chemicals, solvents, and reagents used were of trace metal analysis grade (Sigma-Aldrich, USA). All the containers were thoroughly washed with detergent, soaked in a 10% solution of $HNO_3$ overnight, rinsed with deionized water, and dried in an oven before use. Sediment traps were also conditioned with dilute nitric acid and rinsed with distilled water before use.

### 2.5 Statistical analysis

Using Statistica version 7.1 software, one-way analysis of variance (ANOVA) was carried out to assess variations in metal concentrations in the sedimentation particles, and two-sided Pearson correlations were also performed to examine linear relationships between the measured metals. Descriptive statistics such as means, standard deviations and standard errors were calculated in Microsoft Excel 2010 at a 95% confidence level.

### 2.6 Data analysis

Particle sedimentation fluxes (*Fs*), with units of g/m$^2$/d, were estimated using:

$$F_S = \frac{M}{A} \times D \tag{1}$$

where $M$ is the accumulated dry mass of sedimenting particle (kg) in the sediment trap, $A$ is the cross-sectional area of the sediment trap (m$^2$), and $D$ is the duration of trap deployment (d). Particle-associated metal fluxes (*Fm*, with units of mg/m$^2$/d) were estimated using:

$$F_m = F_S \times C_m \tag{2}$$

where $F_m$ is the flux of metals associated with particles in sedimentation, and $C_m$ is the metal concentration in sedimenting particles (mg/g/day).

The enrichment factor is used to differentiate between anthropogenic and natural inputs of trace metals to a given ecological environment. Sinex and Helz (1981) suggested this normalization method, which is also used in normalizations of the heavy metal content acquired in sedimenting particles in relation to a chosen reference metal, either Fe or Al (Ravichandran et al. 1995). For geochemical normalization, Fe was chosen as the reference metal. The exposure frequency (EF) was calculated using:

$$\mathrm{FE} = \frac{\left(C_I/C_{\mathrm{ref}}\right)_{\mathrm{Sample}}}{\left(S_I/S_{\mathrm{ref}}\right)_{\mathrm{Background}}} \tag{3}$$

where $C_{\mathrm{ref}}$ indicates the Fe concentration in the sedimented particle sample, Ci is the measured heavy metal concentration in the sedimented particle, Si is the local heavy metal background value, and Sref is the Fe concentration measured in the earth's crust. When $0.5 < \mathrm{EF} < 1.5$, this suggests a natural origin of heavy metals. On the other hand, EF>1.5 indicates an anthropogenic origin of heavy metals (Zhang et al. 2007).

Geoaccumulation indices can be used to assess contamination in sedimenting particles, which is done by correlating the current measured concentration of metals with their pre-industrial concentrations. Geoaccumulation index values have been calculated using:

$$I_{\mathrm{geo}} = \log_2\left(\frac{C_n}{1.5 \times B_n}\right) \tag{4}$$

where Cn is the measured concentration of metals in sedimenting particles, and Bn is the geochemical background concentration (Turekian and Wedepohl 1961). Due to lithological variations, a factor of 1.5 has been added to the formula as a background matrix correction factor. The geoaccumulation index ($I_{\mathrm{geo}}$) range comprises seven classes (Solgi et al. 2012): ($I_{\mathrm{geo}} < 0$) uncontaminated; ($0 < I_{\mathrm{geo}} < 1$) uncontaminated to moderately contaminated; ($1 < I_{\mathrm{geo}} < 2$) moderately contaminated; ($2 < I_{\mathrm{geo}} < 3$) moderately to heavily contaminated; ($3 < I_{\mathrm{geo}} < 4$) heavily contaminated; ($4 < I_{\mathrm{geo}} < 5$) heavily to very heavily contaminated; and ($5 < I_{\mathrm{geo}}$) very heavily contaminated.

### 2.7 Potential ecological risk index $\left(E_r^I\right)$

According to Hakanson (1980), the potential ecological risk index shows the degree of pollution of particles in

sedimentation and is used to determine the pollutant. The ecological risk index $\left(E_r^I\right)$ was calculated using:

$$E_r^I = \mathrm{Tr}_I \times \frac{C_n}{C_{\mathrm{ref}}} \tag{5}$$

where $\mathrm{Tr_I}$ is the toxic response factor, $C_n$ is the metal concentration in the study, and $C_{\mathrm{ref}}$ is the reference value. The $\mathrm{Tr_I}$ coefficients for the elements according to their toxicity are: Hg = 40, Cd = 30, As = 10, Cu = Pb = Ni = 5, Cr = 2, and Zn = 1. The $E_r^I$ value assessed is classified as: $E_r^I < 40$ low; $40 < E_r^I < 80$ moderate; $80 < E_r^I < 160$ notable; $160 < E_r^I < 320$ high; and $320 < E_r^I$ major (Maanan et al. 2015).

### 2.8 Assessment of risks associated with the use of particles in sedimentation

Trace metals associated with sedimentation particles enter the human body through ingestion and dermal absorption of the particles (Kim et al. 2004; De Miguel et al. 2007). The quantity of TMEs ingested and absorbed by a human being per day through the use of sedimented particles is known as the chronic daily intake (CDI) (µg/kg/day). The chronic daily dose by ingestion and dermal absorption is calculated using Eqs. (6) and (7), respectively (Song et al. 2019). Parameter and variable values are presented in Table 2 (Song et al. 2019):

$$\mathrm{DJC_{ing}} = \frac{C \times \mathrm{IR} \times \mathrm{CF} \times \mathrm{EF} \times \mathrm{ED}}{\mathrm{BW} \times \mathrm{AT}} \tag{6}$$

$$\mathrm{DJC_{derm}} = \frac{C \times \mathrm{SA} \times \mathrm{CF} \times \mathrm{AF} \times \mathrm{ABS}}{\mathrm{BW} \times \mathrm{AT}} \tag{7}$$

where $\mathrm{DJC_{ing}}$ is the chronic daily dose by ingestion (oral) and $\mathrm{DJC_{derm}}$ is the chronic daily dose by the cutaneous route.

### 2.9 Non-carcinogenic risk of TMEs in sedimented particles

The contaminant exposure quotient is defined as the quotient of the chronic daily intake (CDI) by the reference dose (RfD) for each chemical element based on each exposure route (water ingestion and dermal absorption), as indicated by Eq. (8). Determination of the contaminant exposure quotient (DQ) is used to determine non-carcinogenic risks (Wang et al. 2015):

$$\mathrm{QD_{ing/derm}} = \frac{\mathrm{DJC_{in/derm}}}{\mathrm{RfD_{in/derm}}} \tag{8}$$

**Table 2** Description of input parameters for health risk assessment of selected metals in the sediments (USEPA 2004; Song et al. 2019)

| Parameters | Units | Value | Reference |
|---|---|---|---|
| Metal concentration | µg/g | – | This study |
| Ingestion rate (IR) | mg/j | 114 | Iqbal et al. (2013) |
| Exposure frequency (EF) | J/an | 365 | Iqbal et al. (2013) |
| Frequency duration (ED) | An | 51 | Iqbal et al. (2013) |
| Body weight (BW) | kg | 58.6 | Iqbal et al. (2013) |
| Averaging time (AT) | Jour | 18,615 | Iqbal et al. (2013) |
| Exposed skin area (SA) | $cm^2$ | 5700 | Song et al. (2019) |
| Exposure time (ET) | h/j | 0.6 | USEPA (2004) |
| Adherence factor (AF) | mg/ $cm^2$ | 0.07 | Song et al. (2019) |
| Dermal absorption factor (ABS) | – | 0.001 | Song et al. (2019) |
| Conversion factor (FC) | kg/mg | 0.000006 | Song et al. (2019) |
| Permeability coefficient skin (Kp) | | | |
| Fe | | 0.001 | USEPA (2004) |
| Hg | | 0.001 | USEPA (2004) |
| Cu | cm/h | 0.001 | USEPA (2004) |
| As | | 0.001 | USEPA (2004) |
| Cd | | 0.001 | USEPA (2004) |
| Pb | | 0.004 | USEPA (2004) |

where CDI is the chronic daily dose (µg/kg/d) and RfD is the reference dose of TMEs under a given condition (µg/kg/day). The reference dose by ingestion of particles (RfDin) was obtained from the Iqbal et al. (2013). RfD by dermal absorption (RfD derm) is determined from RfDin multiplied by a gastrointestinal absorption factor (Wang et al. 2015). If the QD value is close to or equal to 1, this indicates potentially adverse effects on human health or the need for further investigation. DQ values > 1 suggest even higher probabilities of adverse health effects (Wang et al. 2015).

The toxicity index (HI) is used to assess the health risk due to the interaction of TMEs present in sedimenting particles. Recent studies suggest that contamination by several metals may cause them to interact, leading to an addition of their toxicity (Taiwo and Awomeso 2017; Song et al. 2019). Thus, the non-carcinogenic risks (DQs) of the various TMEs can add up via the oral or dermal route (HIin and HIderm, respectively) (Wang et al. 2015) to result in an even higher risk. The oral and dermal toxicity index of sedimenting particles was calculated from:

$$\mathrm{HI} = \sum_{I=1}^{n} \left(\mathrm{QD_{ing}} + \mathrm{QD_{derm}}\right) \tag{9}$$

where $\mathrm{QD}_I$ is the exposure quotient for element $I$. When HI < 1, it would have no adverse effects, while for HI > 1 adverse effects could occur (Iqbal et al. 2013).

### 2.10 Carcinogenic risk of TMEs in sedimented particles

Carcinogenic risk (CR) is the probability of an individual developing cancer after a long lifetime (typically 51 years) as a result of exposure to the carcinogenic potential. Linearly, Eq. (10) for low-dose carcinogenic risk is expressed as:

$$CR = DJC \times SF \quad (10)$$

where CDI is the chronic daily dose (mg/kg/day) and SF $(mg/kg/day)^{-1}$ is the slope factor (Table 3).

If a site has multiple carcinogenic contaminants, the cancer risk values for each pollutant and exposure route are summed and compared with the accepted risks. Carcinogenic risks of the order of $1.10^{-6}$ to $1.10^{-4}$ are typically deemed acceptable by Ustaoglu and Islam (2020), according to whom the CR must be less than $1.10^{-6}$. The sum total carcinogenic risk for particulate matter (LCR) according to Ustaoglu and Islam (2020) is determined by:

$$\sum CR = LCR = \left(CR_{ing} + CR_{derm}\right) \quad (11)$$

## 3 Results and Discussion

### 3.1 Sedimentation particle concentrations of As, Cd, Pb, Hg and Fe

The arsenic concentrations of sedimented particles in the estuary of the Comoé, Bia, and Tanoé rivers are shown in Fig. 2. Mean arsenic concentrations ranged from 1.18 ± 0.63 µg/g in the rainy season to 2.21 ± 0.69 µg/g in the flood season in the Comoé River; from 1.14 ± 0.82 µg/g in the rainy season to 2.63 ± 0.62 µg/g in the flood season in the Bia river; and from 0.36 ± 0.34 µg/g in the rainy season to 2.36 ± 0.28 µg/g in the flood season in the Tanoé river.

The mean cadmium concentrations varied from 0.15 ± 0.04 µg/g in the dry season to 0.63 ± 0.21 µg/g in the rainy season in the Comoé River; from 0.16 ± 0.05 µg/g in the dry season to 0.48 ± 0.27 µg/g in the rainy season in the Bia river; and from 0.16 ± 0.06 µg/g in the dry season to 0.30 ± 0.29 µg/g in the rainy season in the Tanoé river (Fig. 3).

Average lead concentrations ranged from 0.45 ± 0.10 µg/g in the rainy season to 1.20 ± 0.72 µg/g in the flood season in the Comoé River; from 0.31 ± 0.18 µg/g in the rainy season to 1.18 ± 0.29 µg/g in the flood season in the Bia river; and from 0.21 ± 0.19 µg/g in the rainy season to 1.20 ± 0.16 µg/g in the flood season in the Tanoé river (Fig. 4).

Mercury concentrations in sedimented particles showed spatial and temporal variability, with mean values ranging from 0.26 ± 0.25 µg/g in the rainy season to 0.71 ± 0.47 µg/g in the flood season in the Comoé River; from 0.58 ± 0.32 µg/g in the flood season to 0.64 ± 0.61 µg/g in the rainy season in the Bia river; and from 0.28 ± 0.53 µg/g in the rainy season to 0.82 ± 0.60 µg/g in the rainy season in the Tanoé river (Fig. 5).

Finally, mean iron concentrations ranged from 20,405.66 ± 3596.07 µg/g in the dry season to 24,446.02 ± 2258.41 µg/g in the rainy season in the Comoé River; from 18,553.35 ± 11,164.18 µg/g in the rainy season to 21,976.96 ± 2890.21 µg/g in the dry season in the Bia river; and from 18,124.94 ± 9959.56 µg/g in the rainy season to 20,522.84 ± 4492.76 µg/g in the dry season in the Tanoé river (Fig. 6).

However, ANOVA revealed no significant difference between mean concentrations of arsenic, cadmium, lead, mercury, and iron at $p < 0.05$. The results show that 60%, 73.33%, and 53.33% of As samples, 93.33%, 93.33%, and 80% of Cd samples, and 86.66%, 86.66%, and 80% of Hg samples in the Comoé, Bia, and Tanoé rivers have concentrations above that of the UCC (2 µg/g for As, 0.101 µg/g for Cd, and 0.056 µg/g for Hg). The high concentrations of As, Cd, and Hg recorded could be attributed to anthropogenic activities such as gold mining and agricultural activities. The sampling stations on the Comoé, Bia, and Tanoé rivers are located in agricultural areas with industrial plantations of cocoa, coffee, rubber, and oil palm. Thus, leaching from these agricultural lands could release fertilizers and pesticides into the three rivers (Chai et al. 2017; Zhang et al. 2018; Ouattara et al. 2018) leading to high concentrations of Cd and As. In the watersheds of the rivers, the mercury amalgamation technique is used to extract the gold. This method produces enormous quantities of mercury in these rivers, a finding which corroborates those of Asare-Donkor and Adimado (2016) and Adjei-Kyereme et al. (2015), who have indicated that gold panning activities contribute significantly to the release of mercury into Ghana's rivers. Similarly, the abusive use of charcoal as a substitute for domestic gas, which is in short supply in very isolated rural areas, is a major factor increasing mercury concentration levels. In addition, during the gold extraction process in the study

**Table 3** Standard values for calculating carcinogenic risk (CR) (US EPA 2011, 2012)

| Metals | SF $(mg\ kg^{-1}\ j^{-1})^{-1}$ | | RfD $(\mu g\ kg^{-1}\ j^{-1})$ | |
|---|---|---|---|---|
| | Oral | Dermal | Oral | Dermal |
| Cd | 6.500 | NA | 0.5 | 0.025 |
| Hg | NA | NA | 0.3 | 0.3 |
| As | 1.5 | NA | 0.3 | 0.3 |
| Pb | 8.5 | NA | 1.4 | 0.42 |
| Fe | NA | NA | 700 | 140 |

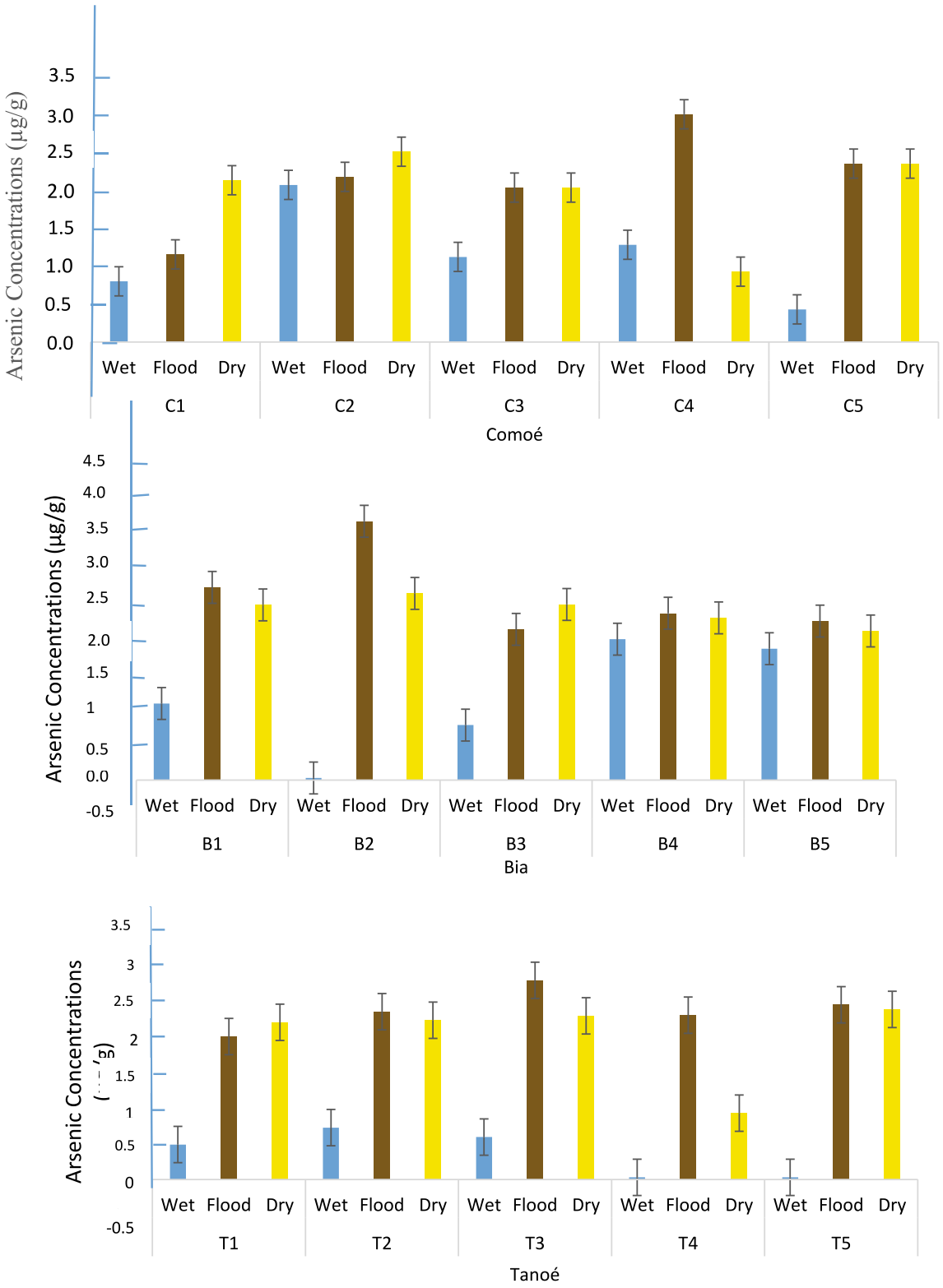


**Fig. 2** Total arsenic concentrations (µg/g) in the Comoé, Bia, and Tanoe Rivers during the rainy, flood, and dry seasons

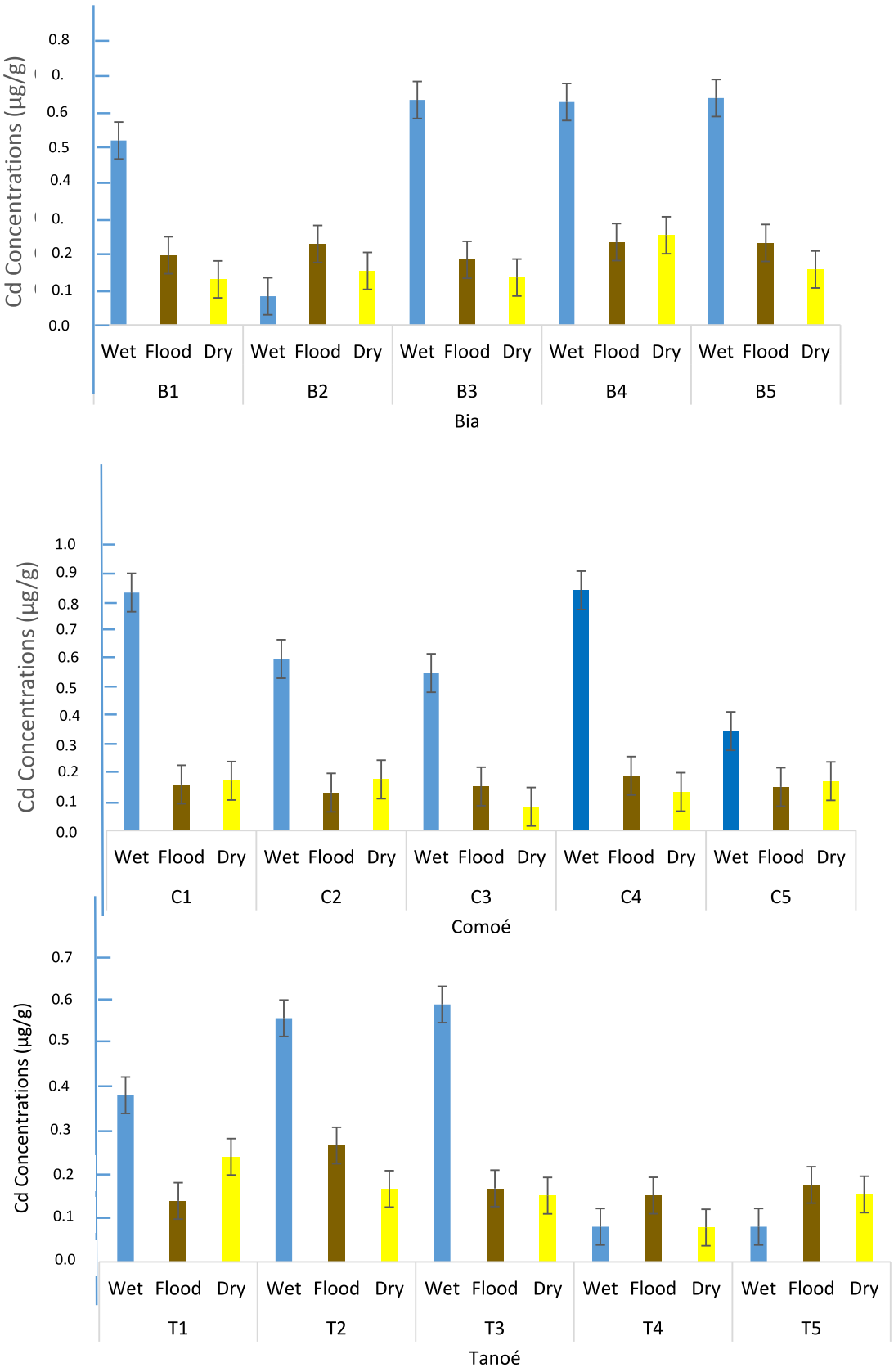


**Fig. 3** Total cadmium concentrations (µg/g) in the Bandama, Comoé, and Bia Rivers during the dry, rainy, and flood seasons

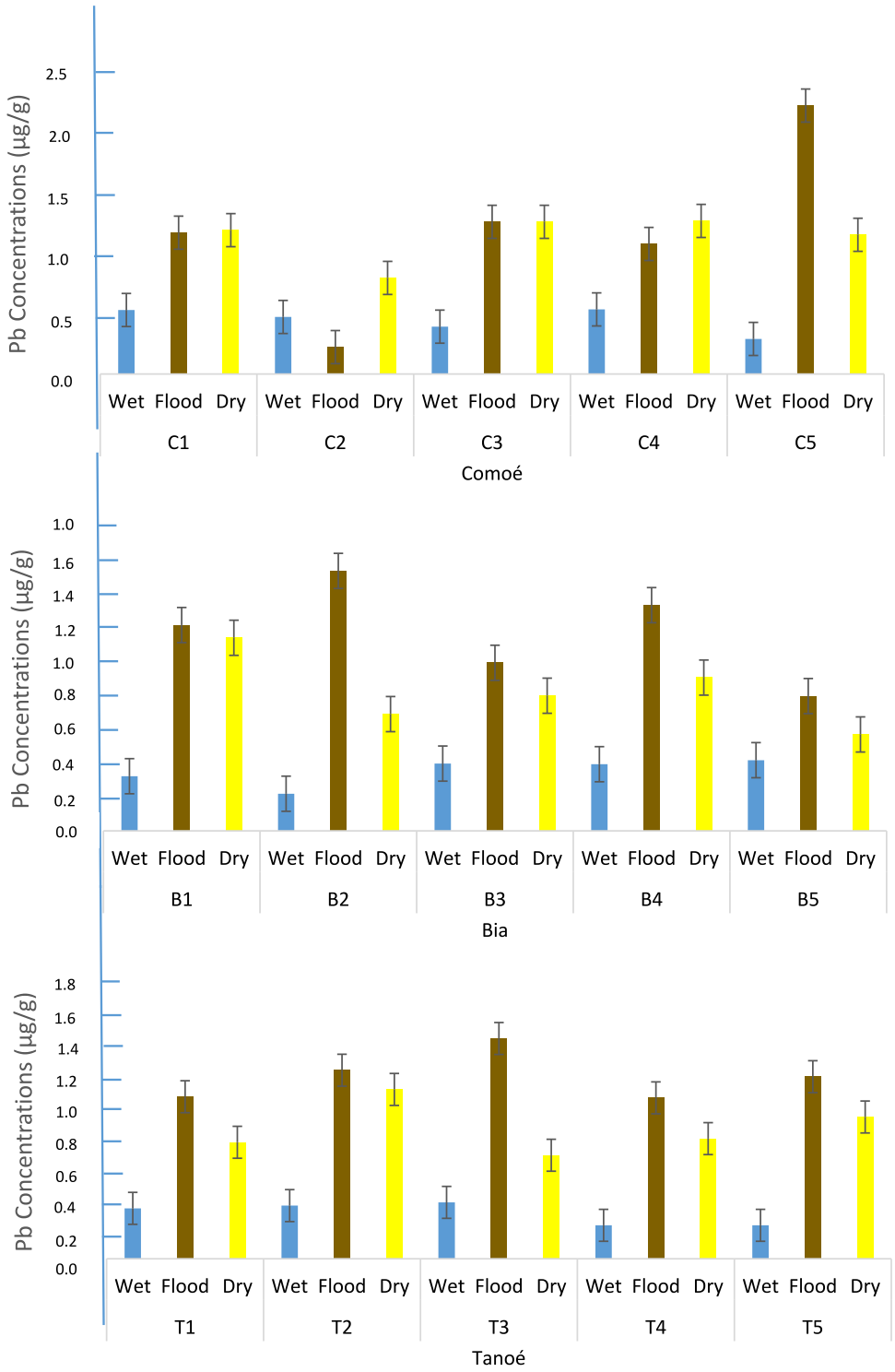


**Fig. 4** Total lead concentrations (µg/L) in the Bandama, Comoé, and Bia Rivers during the dry, rainy, and flood seasons

area, cyanide is used to leach gold ores, resulting in high arsenic concentrations in the three rivers, as mentioned by Samouhos et al (2021). The highest concentrations of As, Cd, Pb, Hg, and Fe were obtained during the flood and rainy seasons, confirming that runoff water is a transport vector for the metals Cd, Pb, Hg, and Fe in the rivers. It has been reported that vehicle exhaust containing leaded petrol has been reported to be a source of Pb in the environment (Lü et al. 2018). Shipping and fishing activities are also carried out in the study area using motorboats. Consequently, the presence of Pb in the sedimentation particles may be due to maritime and fishing activities.

Concentrations of As, Pb, Cd, Hg, and Fe in sedimented particles in the estuary of the Comoé, Bia, and Tanoé rivers

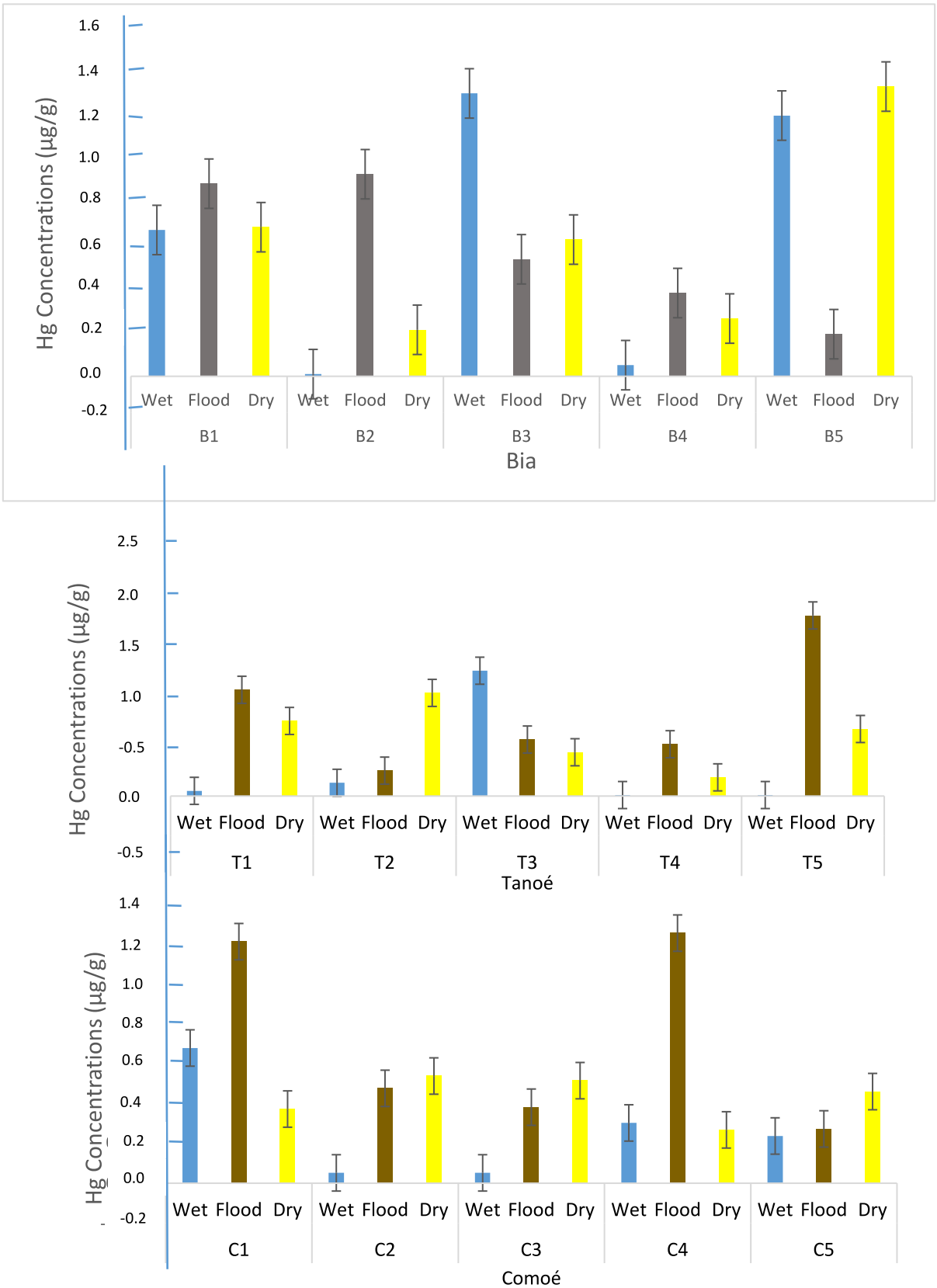


**Fig. 5** Total mercury concentrations (µg/L) in the Bandama, Comoé, and Bia Rivers during the dry, rainy, and flood seasons

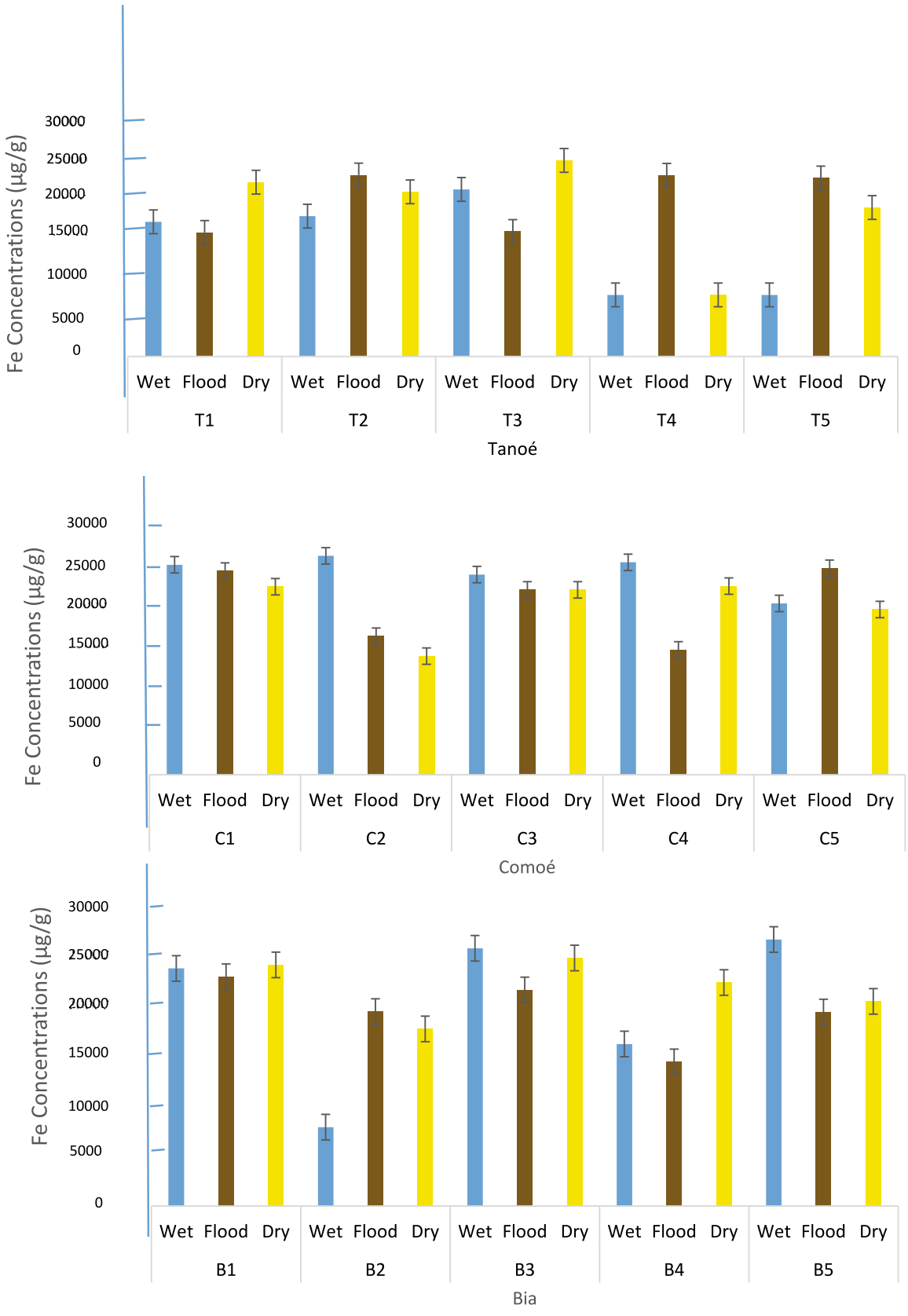


**Fig. 6** Total iron concentrations (µg/L) in the Bandama, Comoé, and Bia Rivers during the dry, rainy, and flood seasons

have also been compared with those of other studies worldwide (Table 4).

The concentrations of As, Pb, Cd, Hg, and Fe in sediment particles in this study are lower than the values reported by Arambarri et al. (2003) in particles from the Gipuzkoa River in Spain, by Ghani et al. (2013) in Egypt in particles from Abu-Oir Bay, by Luo et al. (2010) in the Bohai and Yellow River in China, with the exception of mercury, by Vallius et al. (2007) in the Gulf of Finland, and by Botwe et al. (2017) in Ghana in Tema Harbour. Similarly, concentrations are lower than those reported by Al-Tanni et al. (2014) in the Gulf of Aqaba in Saudi Arabia, with the exception of cadmium and iron, whereas the concentrations of As, Cd, Pb, Hg, and Fe in sediment particles obtained in this study are higher than those of Rumisha et al. (2012) in Tanzania on the Salaam coast. In view of the above, the concentrations obtained in this study are within the range of concentrations observed elsewhere in the world.

### 3.2 Correlation between trace metals

Correlation coefficients were calculated to determine the relationships between trace metals (Table 5). Correlation is considered moderate when $0.5 < r < 0.7$, whereas $r > 0.7$ indicates a strong correlation according to Shil and Singh (2019). A moderate correlation was observed between Fe and Cd ($r = 0.52$) in the Comoé River, while As was significantly correlated with Pb ($r = 0.80$), Fe was moderately correlated with Hg ($r = 0.61$) in the Bia River. In the Tanoe River, Pb was strongly correlated with arsenic ($r = 0.86$). Fe correlated with Cd in the Comoé and Hg in the Bia demonstrate that Cd and Hg are of natural origin, mainly weathering processes in the three rivers. This also suggests that the distributions of Cd in the Bia and Hg in the Comoé are driven by iron oxides and hydroxides (Kinimo et al. 2018). Furthermore, the strong correlations between As and Pb

**Table 4** Comparison of mean trace elements concentrations (mean ± standard deviation) with those reported in other rivers located in other regions in settling particles

| Fleuves | As | Cd | Pb | Hg | Fe | References |
|---|---|---|---|---|---|---|
| Wet (Comoé, Bia, et Tanoé) | 0.89 ± 0.70 | 0.47 ± 0.28 | 0.32 ± 0.18 | 0.39 ± 0.49 | 18,124 ± 9959 | Present study |
| Flood (Comoé, Bia, et Tanoé) | 2.40 ± 0.55 | 0.18 ± 0.04 | 1.19 ± 0.42 | 0.70 ± 0.45 | 20,231 ± 3689 | Present study |
| Dry (Comoé, Bia, et Tanoé) | 2.15 ± 0.52 | 0.16 ± 0.05 | 0.94 ± 0.23 | 0.55 ± 0.31 | 20,522 ± 4492 | Present study |
| Tema Harbour (Ghana) | 146–1470 | – | 20.3–229 | 0.1–3 | 33,290–65,920 | Botwe et al. (2017) |
| Gipuzkoa (Espagne) | – | 0.22–12.34 | 55–711 | – | 10,700–43,000 | Arambarri et al. (2003) |
| Abu-Qir Bay (Egypt) | 1.60–8.67 | 0.31–4.89 | 1.90–16.79 | – | 90–35,890 | Ghani et al. (2013) |
| Salaam coast (Tanzania) | 0.2–1.3 | 0.01–0.04 | 0.75–2.20 | – | 461–5352 | Rumisha et al. (2012) |
| Northern Bohai and Yellow Seas (China) | 5.6–13 | 0.050–0.83 | – | 0.020–0.18 | – | Luo et al. (2010) |
| Gulf of Aqaba (Saudi Arabia) | 15.1 | 0.07 | 3.72 | 2.37 | 1437 | Al-Taani et al. (2014) |
| Gulf of Finland | 7.25–19.1 | 0.84–2.69 | 37.3–58.9 | 0.09–0.30 | – | Vallius et al. (2007) |

**Table 5** Correlation matrix of metal and TOC concentrations in settling particles

| | | As | Cd | Pb | Hg | Fe |
|---|---|---|---|---|---|---|
| Comoe river | As | 1.00 | | | | |
| | Cd | − 0.47 | 1.00 | | | |
| | Pb | 0.39 | − 0.55 | 1.00 | | |
| | Hg | 0.25 | − 0.26 | 0.18 | 1.00 | |
| | Fe | − 0.53 | **0.52** | 0.11 | − 0.38 | 1.00 |
| Bia river | As | 1.00 | | | | |
| | Cd | − 0.68 | 1.00 | | | |
| | Pb | **0.80** | − 0.67 | 1.00 | | |
| | Hg | − 0.22 | 0.19 | − 0.11 | 1.00 | |
| | Fe | − 0.38 | 0.23 | − 0.31 | **0.61** | 1.00 |
| Tanoe river | As | 1.00 | | | | |
| | Cd | − 0.69 | 1.00 | | | |
| | Pb | **0.86** | − 0.71 | 1.00 | | |
| | Hg | 0.32 | − 0.09 | 0.31 | 1.00 | |
| | Fe | 0.42 | 0.15 | 0.07 | 0.33 | 1.00 |

Numbers in bold (large, thick type) denote statistically significant relationships between metals

in the Bia and Pb and As in the Tanoé may indicate similar sources of these metals, mainly from gold mining and agricultural uses of fertilizers and pesticides (Ouattara et al. 2018).

### 3.3 Enrichment factor

The enrichment factor values calculated for the metals As, Cd, Pb and Hg in the estuary of the Comoé, Bia and Tanoé rivers are shown in Fig. 7. Enrichment factor values for As range from 0.9 (C1) to 2.8 (C2). Cd values range from 2.5 (T5) to 7 (B4), Pb enrichment factor values range from 0.05 (B5) to 0.10 (T4), and enrichment factor values for Hg range from 7 (B4) to 22 (B5). The enrichment factor values calculated for Pb and As (with the exception of stations B2, B4, C4, B6, and T3) are below 1.5, proving that Pb has a natural origin. As, on the other hand, has both a geogenic origin and minimal enrichment. This trend could be explained by the contribution of natural products to the detriment of agrochemicals using Pb and As in agriculture. Also, the low level of industrialization in the estuary of the three rivers could be the cause of the natural origin of Pb and As. Furthermore, the enrichment factor values determined for Cd and Hg are greater than 1.5, indicating that Cd and Hg are of anthropogenic origin. Intense mining activity downstream and upstream of the rivers is believed to be responsible for the high Hg concentrations recorded. Anthropogenic Cd could probably come from fertilizers and pesticides used in agriculture. Domestic wastewater discharges in the Comoé, Bia and Tanoé rivers could also be responsible for the high Cd concentrations (Islam et al. 2015).

### 3.4 Distributions and fluxes of particles associated metals in the Comoe, Bia and Tanoe river

Figure 8 shows that the highest fluxes were obtained during the flood season in the Bia and Tanoé rivers, and during the rainy season in the Comoé. Station C5 recorded an As flux of 737.48 μg/m$^2$/d in the Comoé river, station B1 recorded an As flux of 3037.98 μg/m$^2$/d in the Bia, and station T2 recorded an As flux of 8028.08 μg/m$^2$/d in the Tanoe river.

With regard to Cd, the highest fluxes were obtained during the rainy season in the Comoé and Bia rivers and during the flood season in the Tanoé river: station C5 recorded a Cd flux of 46.11 μg/m$^2$/d in the Comoé river; station B5 recorded a Cd flux of 258.64 μg/m$^2$/d in the Bia river; and station T2 recorded a Pb flux of 909.7 μg/m$^2$/d in the Tanoé river.

Also, for Pb, the highest fluxes were obtained during the flood season: station C5 recorded a Pb flux of 679.9 μg/m$^2$/d in the Comoé river; station B1 recorded a Pb flux of 1356.7 μg/m$^2$/d in the Bia; and station T2 recorded a Pb flux of 4260.1 μg/m$^2$/d in the Tanoé river.

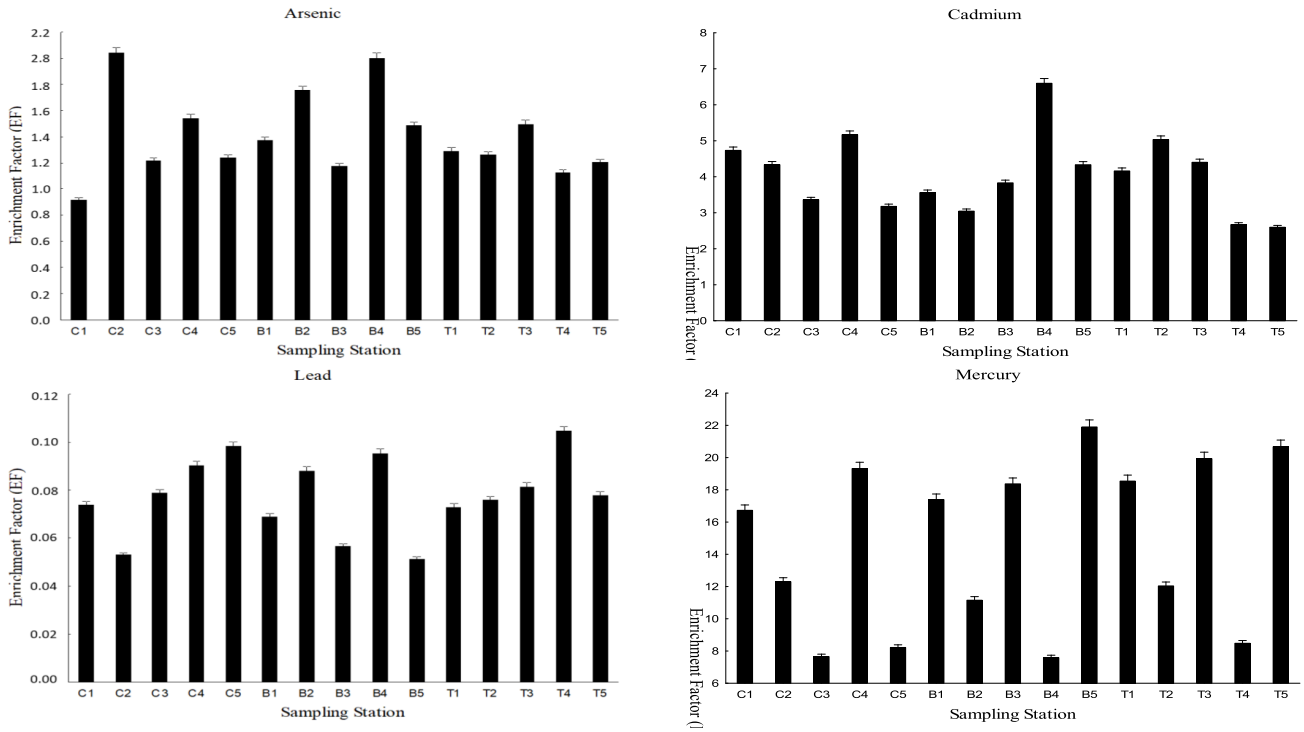


**Fig. 7** Enrichment factor mean values of the analyzed metals and their standard deviations

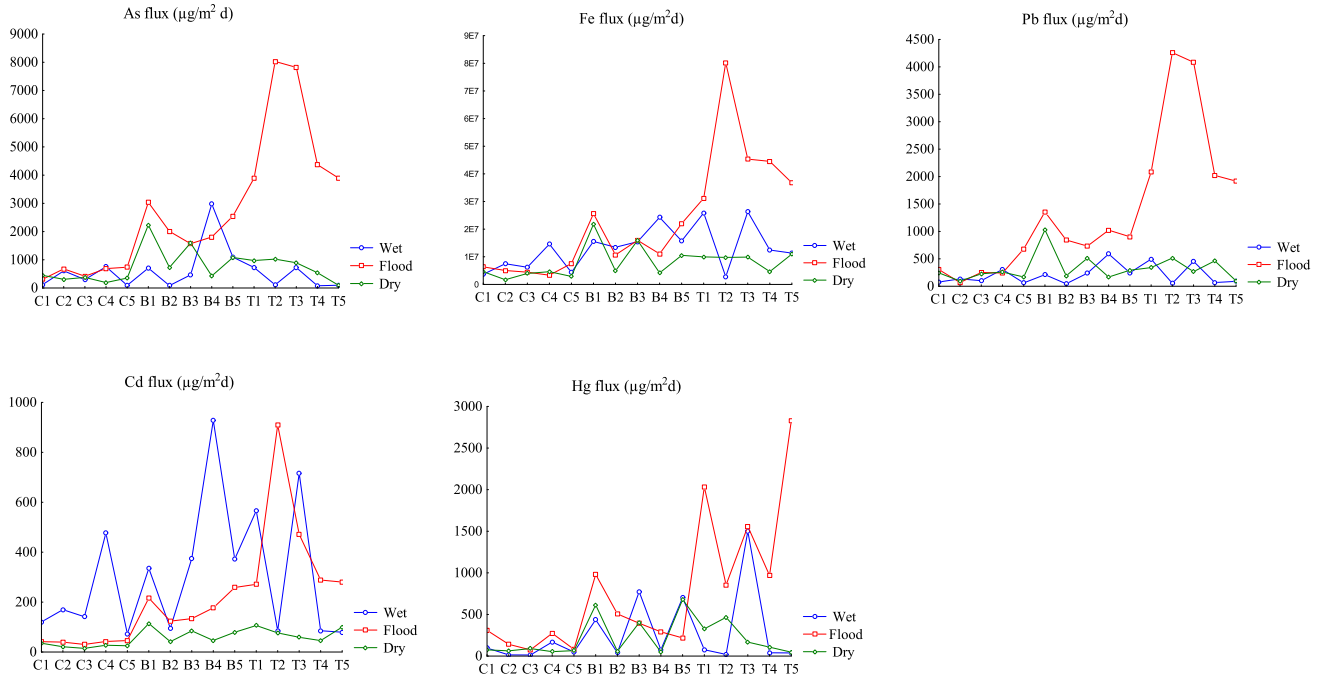


**Fig. 8** Estimated daily settling fluxes of suspended particles and associated metals at different sampling stations over the three seasons (wet, flood, and dry) in the Comoé, Bia, and Tanoé rivers

For Hg, the highest fluxes were obtained during the flood season: station C1 recorded a Pb flux of 309.1 µg/m$^2$/d in the Comoé river; station B2 recorded a Pb flux of 506.8 µg/m$^2$/d in the Bia; and station T5 recorded a Pb flux of 2828.9 µg/m$^2$/d in the Tanoé river.

As for Fe, the highest fluxes were obtained during the flood season in the Bia and Tanoé rivers and during the rainy season in the Comoé: station C5 recorded a Pb flux of 7,572,937.7 µg/m$^2$/d in the Comoé river; station B1 recorded a Pb flux of 25,618,945.9 µg/m$^2$/d in the Bia; and station T5 recorded a Pb flux of 80,215,344.9 µg/m$^2$/d in the Tanoé river.

Lead fluxes, As fluxes, Hg fluxes, and iron fluxes are all very high during the flood season. Cd fluxes are high during the rainy season for the Bia and Comoé rivers, and during the flood season for the Tanoé river. The highest fluxes of metals associated with sedimenting particles were recorded on the Tanoé during the flood season. This may be due to the depth of the river, high flow creating sediment resuspension, strong erosion and heavy mining activity carried out further upstream in Ghana on the Tanoé River (Nyantakyi et al. 2019; Botwe et al. 2017). The curves in Fig. 8 are represented in a sawtooth pattern, demonstrating that there are no clear trends in the evolution of flows from upstream to downstream rivers. This indicates both local and upstream inputs to the estuary of the Comoé, Bia, and Tanoé rivers. These observations therefore confirm the input of the metals As, Cd, Pb, Hg, and Fe into the Ebrié and Aby lagoons during the flood and rainy seasons via runoff. These flux values show a strong direct interaction observed between sediment particles (metal-bound fine fraction) and metal fluxes. This strong interaction indicates that metal transport at depth and its distribution in the three rivers are well regulated by the settling of sedimented particles (metal-bound fine fraction). This can be attributed to strong interactions between the metals and the settling particles in the water column (Horowitz et al. 1989; Hostache et al. 2014). As sedimented particles (silts and clays) are naturally enriched in Fe, the distribution of metals in rivers is possible thanks to iron oxides and hydroxides. This is in line with Table 5, which shows a moderate correlation between trace metals (Hg, Cd) and Fe. The flux results obtained are higher than those of Botwe et al. (2017); a difference resulting from the different sampling sites.

## 3.5 Sedimentation particle quality guides

### *3.5.1 Geoaccumulation indices*

The geoaccumulation index values calculated for As, Cd, Pb, and Hg sedimentation particles in the estuary of the Comoé, Bia, and Tanoé rivers are shown in Fig. 9.

The calculated values indicated variable geoaccumulation index levels in the Comoé, Bia, and Tanoé rivers. For As and Pb, the calculated geoaccumulation index values were below

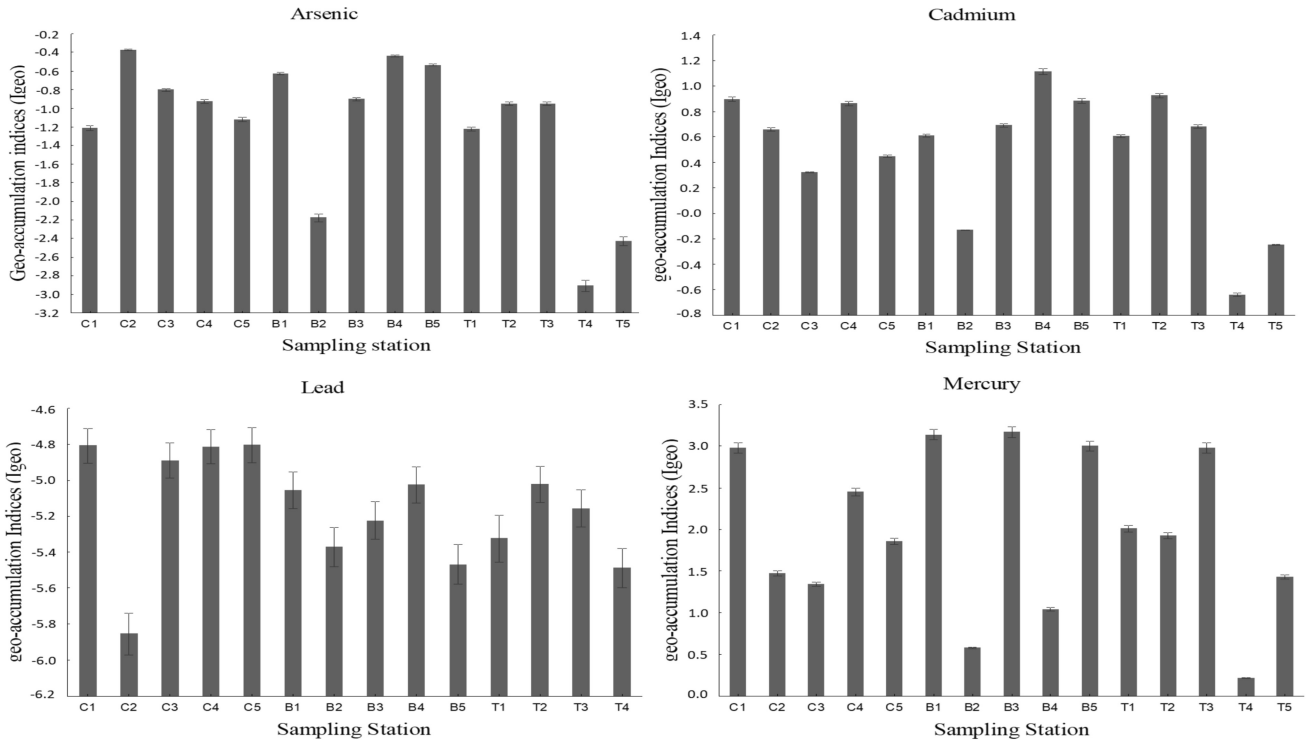


**Fig. 9** Geo-accumulation indices mean values of the analyzed metals and their standard deviations

0 for all three rivers, suggesting that the sediment particles at the sampled stations are uncontaminated with As and Pb.

Concerning Cd, sedimentation particles from the sampled stations are uncontaminated to moderately contaminated with Cd indicated by geoaccumulation index values of $0 < I_{géo} < 1$, except for particles at station B4 which are moderately contaminated with Cd, whose calculated geoaccumulation index values are greater than 1.

For Hg, sedimentation particles from stations T4, B4, and B2 are uncontaminated to moderately contaminated indicated by geoaccumulation index values of $0 < I_{geo} < 1$, sediment particles at stations C5, T1, T2, and T5 are moderately contaminated with Hg ($1 < I_{geo} < 2$), and, for stations C1 and T3 with geoaccumulation index values between 2 and 3, sedimentation particles are moderately to heavily contaminated. At stations B1, B3, and B5, the particles are highly contaminated, as indicated by geoaccumulation index values of $3 < I_{geo} < 4$.

The accumulation of Cd and Hg in sediment particles in the Comoé, Bia, and Tanoé rivers may be due to domestic wastewater, fishing, agriculture, bush fires, and mining.

### *3.5.2 Ecological risk indexes*

In order to show the degree of pollution at an ecological level, the potential ecological risk index of sedimented particles containing As, Cd, Pb, and Hg was determined, and the values are shown in Table 6.

**Table 6** Potential ecological risk ($E_r^I$) values for trace elements in settling particles

| Sampling | ERI | | | | PERI |
|---|---|---|---|---|---|
| | As | Cd | Pb | Hg | |
| C1 | 0.94 | 11.63 | 0.07 | 118.72 | 131.36 |
| C2 | 1.55 | 9.08 | 0.04 | 55.91 | 66.58 |
| C3 | 1.19 | 7.85 | 0.07 | 49.74 | 58.85 |
| C4 | 1.20 | 11.62 | 0.07 | 95.75 | 108.64 |
| C5 | 1.18 | 6.70 | 0.09 | 50.85 | 58.82 |
| B1 | 1.40 | 8.36 | 0.06 | 119.20 | 129.03 |
| B2 | 1.41 | 4.57 | 0.06 | 61.25 | 67.29 |
| B3 | 1.20 | 9.42 | 0.05 | 131.07 | 141.74 |
| B4 | 1.48 | 11.04 | 0.06 | 37.16 | 49.74 |
| B5 | 1.38 | 10.17 | 0.04 | 144.74 | 156.33 |
| T1 | 1.04 | 7.57 | 0.05 | 97.34 | 106.00 |
| T2 | 1.17 | 9.85 | 0.06 | 74.01 | 85.10 |
| T3 | 1.25 | 9.03 | 0.06 | 117.75 | 128.10 |
| T4 | 0.72 | 3.09 | 0.05 | 37.34 | 41.20 |
| T5 | 1.07 | 4.08 | 0.06 | 129.76 | 134.98 |

The results of the potential ecological risk indices calculated for As, Cd, and Pb show $E_r^I$ values below 40 at all the stations, suggesting their low level of potential ecological risk. Only

**Table 7** Description of health risk evaluation for PTEs in settling particles

| | | RfD (µg/kg/day) | | Exposure assessment | | Non-carcinogenic-risk | | | Carcinogenic risk | | | |
|---|---|---|---|---|---|---|---|---|---|---|---|---|
| | | Oral | Dermal | $Exp_{ing}$ | $Exp_{derm}$ | $HQ_{ing}$ | $HQ_{derm}$ | HI | SF (mg/kg/day) | $CR_{ing}$ | $CR_{der}$ | LCR |
| Comoe river | As | 0.3 | 0.3 | 2.12E−05 | 7.42E−08 | 7.06E−02 | 2.47E−04 | 7.09E−02 | 1.50E+00 | 3.18E−05 | 1.11E−07 | 3.19E−05 |
| | Cd | 0.5 | 0.025 | 3.65E−06 | 1.28E−08 | 7.30E−03 | 5.11E−04 | 7.81E−03 | 6.30E+00 | 2.30E−05 | 8.04E−08 | 2.31E−05 |
| | Pb | 1.4 | 0.42 | 1.08E−05 | 3.80E−08 | 7.74E−03 | 9.04E−05 | 7.84E−03 | 8.50E−03 | 9.22E−08 | 3.23E−10 | 9.25E−08 |
| | Hg | 0.3 | 0.3 | 5.41E−06 | 1.89E−08 | 1.80E−02 | 6.31E−05 | 1.81E−02 | | | | |
| | Fe | 700 | 140 | 2.55E−01 | 8.93E−04 | 3.64E−01 | 6.38E−03 | 3.71E−01 | | | | |
| HI | | | | | | | | 4.75E−01 | | | | |
| Bia river | As | 0.3 | 0.3 | 2.41E−05 | 8.42E−08 | 8.02E−02 | 2.81E−04 | 8.05E−02 | 1.50E+00 | 3.61E−05 | 1.26E−07 | 3.62E−05 |
| | Cd | 0.5 | 0.025 | 3.39E−06 | 1.19E−08 | 6.78E−03 | 4.74E−04 | 7.25E−03 | 6.30E+00 | 2.13E−05 | 7.47E−08 | 2.14E−05 |
| | Pb | 1.4 | 0.42 | 9.15E−06 | 3.20E−08 | 6.54E−03 | 7.63E−05 | 6.61E−03 | 8.50E−03 | 7.78E−08 | 2.49E−15 | 7.78E−08 |
| | Hg | 0.3 | 0.3 | 7.20E−06 | 2.52E−08 | 2.40E−02 | 8.40E−05 | 2.41E−02 | | | | |
| | Fe | 700 | 140 | 2.40E−01 | 8.41E−04 | 3.43E−01 | 6.01E−03 | 3.49E−01 | | | | |
| HI | | | | | | | | 4.68E−01 | | | | |
| Tanoe river | As | 0.3 | 0.3 | 1.84E−05 | 6.44E−08 | 6.14E−02 | 2.15E−04 | 6.16E−02 | 1.50E+00 | 2.76E−05 | 1.78E−12 | 2.76E−05 |
| | Cd | 0.5 | 0.025 | 2.62E−06 | 9.16E−09 | 5.23E−03 | 3.66E−04 | 5.60E−03 | 6.30E+00 | 1.65E−05 | 1.51E−13 | 1.65E−05 |
| | Pb | 1.4 | 0.42 | 9.17E−06 | 3.21E−08 | 6.55E−03 | 7.64E−05 | 6.63E−03 | 8.50E−03 | 7.79E−08 | 2.50E−15 | 7.79E−08 |
| | Hg | 0.3 | 0.3 | 6.66E−06 | 2.33E−08 | 2.22E−02 | 7.77E−05 | 2.23E−02 | | | | |
| | Fe | 700 | 140 | 2.10E−01 | 7.36E−04 | 3.00E−01 | 5.26E−03 | 3.06E−01 | | | | |
| HI | | | | | | | | 4.02E−01 | | | | |

Hg gives three pollution levels of ecological risk index. The first level involves stations B4 and T3, which show low contamination indicated by $E_r^I < 40$ values. Then the second level involves stations B2, C2, C3, C5, and T2, which show moderate contamination thanks to values $40 < E_r^I < 80$. Finally the third level involves stations B1, B3, B5, C1, C4, T1, T3, and T5, and the potential ecological risk values ($80 < E_r^I < 160$) for these stations show noticeable Hg particle contamination. These results show the advanced degradation of the Comoé, Bia, and Tanoé rivers due to the impact of mining activities upstream and downstream of the Comoé, Bia, and Tanoé rivers.

### 3.6 Human health risk assessment

QD and HI values > 1 indicate adverse health effects resulting from the presence of TMEs in sedimented river particles. The results of the present study showed that the QDderm, QDing, and HI values of trace metals from sediment particles were < 1 (Table 7), suggesting that there are no health problems other than cancer. Also, the non-carcinogenic health risk for the ingestion route of exposure was higher than that for skin contact, showing that the ingestion route makes a greater contribution to the potential health risks from TME-contaminated sediment particles. In addition, HI values for the elements were ranked in descending order: Fe > As > Hg > Pb > Cd, for the Comoé and Tanoé rivers, and Fe > As > Hg > Cd > Pb for the Bia river. For each river, values were ranked in ascending order as: Tanoé < Bia < Comoé. Given that the HI values are < 1, there are no significant adverse effects on human health from the TMEs. However, similar studies at sites affected by mining activities have reported high potential health risks (Xie et al. 2017).

The lifetime cancer risk (LCR) results for the TMEs (Pb, Cd, and As) are presented in Table 7. A relatively higher CSF value for As than for Cd and Pb (As > Cd > Pb) reveals that As remarkably possesses a higher potential for carcinogenic risk. The calculated LCR values for As were $3.19 \times 10^{-5}$, $3.62 \times 10^{-5}$, $2.76 \times 10^{-5}$ and $2.31 \times 10^{-5}$for the Comoé river, and $2.14 \times 10^{-5}$ and $1.65 \times 10^{-5}$ for Cd for the Bia and Tanoé rivers, respectively. These values ranged from $1.00 \times 10^{-6}$ to $1.00 \times 10^{-4}$ which was the range recommended by the US EPA. Consequently, there are no carcinogenic risks for As and Cd. On the other hand, the LCR values for Pb $9.25 \times 10^{-8}$, $7.78 \times 10^{-8}$ and $7.79 \times 10^{-8}$ , respectively, for the Comoé, Bia, and Tanoé rivers were well below the US EPA's acceptable threshold value ($1.00 \times 10^{-6}$), indicating that there are no significant carcinogenic risks for Pb.

## 4 Conclusion

This study assessed the total concentrations, fluxes, and potential risks from sedimenting particles associated with arsenic, lead, cadmium, mercury, and iron in the estuary of the Comoé, Bia, and Tanoé rivers. Mean arsenic concentrations were 1.82 ± 0.67 µg/g, 2.06 ± 0.61 µg/g, and 1.57 ± 0.90 µg/g for the Comoé, Bia, and Tanoé rivers, respectively. Cadmium concentrations were characterized by peaks of 0.31 ± 0.21 µg/g for the Comoé, 0.29 ± 0.17 µg/g for the Bia, and 0.21 ± 0.13 µg/g, for the Tanoé. Also, mean lead concentrations were 0.93 ± 0.43 µg/g for the Comoé, 0.77 ± 0.35 µg/g for the Bia, and 0.76 ± 0.37 µg/g for the Tanoé. Mean mercury concentrations were 0.93 ± 0.43 µg/g for the Comoé, 0.77 ± 0.35 µg/g for the Bia, and 0.76 ± 0.37 µg/g for the Tanoé. For iron, the averages were 21,857.77 ± 3008.34 µg/g for the Comoé; 21,857.77 ± 4374.73 µg/g for the Bia, and 16,964.36 ± 5981.89 µg/g for the Tanoé. The highest total concentrations were generally observed during the rainy and flood seasons. Total concentrations of arsenic, cadmium, and mercury are above the UCC standard due to anthropogenic activities in the area. Sediment particle fluxes associated with the metals lead, arsenic, mercury, and iron were highest during the flood season in the three rivers, while sedimentation particle fluxes associated with cadmium were highest during the rainy season. Consequently, sediment particles from the three rivers are important sources of cadmium, lead, arsenic, mercury, and iron to the Atlantic Ocean via the Aby and Ebrié lagoons. Pearson correlation analysis and the enrichment factor showed that trace metals came mainly from anthropogenic sources, notably gold mining and agriculture. The contamination indices studied (Igeo, and $E_r^I$) showed that particles from all three rivers are severely contaminated with mercury. However, the results of the assessment of potential risks to human health suggest that there is no likelihood of exposure of the human community to harmful effects and cancer risk through water ingestion. Reducing local and upstream inputs from human activities could mitigate the pollution of sedimenting particles in the river estuaries. It is essential to integrate the information from this study into policy- and decision-making processes for better management of transboundary river water resources in coastal countries, particularly Côte d'Ivoire.

**Acknowledgements** We would like to thank the Centre de Recherche Oceanologique (CRO), the Laboratiore National d'Analyse pour le Développement Agricole (LANADA) in Abidjan and the marine geology laboratory of the UFR STRM of the Université Felix Houphouët-Boigny.

**Author contributions** DNFK: conceptualization, methodology, data curation, formal analysis, funding acquisition, resources, writing- original draft; N'LBK: methodology, supervision, data curation, writing—review and editing, project administration, validation; EAAY: editing, formal analysis; KMY: formal analysis, methodology, funding acquisition. ASC: project administration, supervision.

**Data availability** The datasets used and/or analyzed during the current study are available from the corresponding author on reasonable request.

**Declarations**

**Conflict of interest** The authors declare that they have no known competing financial interests or personal relationships that could have appeared to influence the work reported in this paper.

## References


Adjei-Kyereme Y, Donkor AK, Golow AA, Yeboah PO, Pwamang J (2015) Mercury concentrations in water and sediments in rivers impacted by artisanal gold mining in the Asutifi District, Ghana. Res J Chem Environ 3:40–48

Aldous AR, Tear T, Fernandez LE (2024) The global challenge of reducing mercury contamination from artisanal and small-scale gold mining (ASGM): evaluating solutions using generic theories of change. Ecotoxicology 33(4–5):506–517. https://doi.org/10.1007/s10646-024-02741-3

Al-Taani AA, Batayneh A, Nazzal Y, Ghrefat H, Elawadi E, Zaman H (2014) Status of trace metals in surface seawater of the Gulf of Aqaba, Saudi Arabia. Mar Pollut Bull 86(1–2):582–590. https://doi.org/10.1016/j.marpolbul.2014.05.060

Arambarri I, Garcia R, Millán E (2003) Assessment of tin and butyltin species in estuarine superficial sediments from Gipuzkoa, Spain. Chemosphere 51(8):643–649. https://doi.org/10.1016/S0045-6535(03)00154-1

Asare-Donkor NK, Adimado AA (2016) Influence of mining related activities on levels of mercury in water, sediment and fish from the Ankobra and Tano River basins in South Western Ghana. Environ Syst Res 5(1):5. https://doi.org/10.1186/s40068-016-0055-4

Bastami KD, Neyestani MR, Shemirani F, Soltani F, Haghparast S, Akbari A (2015) Heavy metal pollution assessment in relation to sediment properties in the coastal sediments of the southern Caspian Sea. Mar Pollut Bull 92(1–2):237–243. https://doi.org/10.1016/j.marpolbul.2014.12.035

Botwe BO, Abril JM, Schirone A, Barsanti M, Delbono I, Delfanti R, Nyarko E, Lens PNL (2017) Settling fluxes and sediment accumulation rates by the combined use of sediment traps and sediment cores in Tema Harbour (Ghana). Sci Total Environ 609:1114–1125. https://doi.org/10.1016/j.scitotenv.2017.07.139

Chai LY, Li H, Yang ZH, Min XB, Liao Q, Liu Y, Men SH, Yan YN, Xu JX (2017) Heavy metals and metalloids in the surface sediments of the Xiangjiang River, Hunan, China: distribution, contamination, and ecological risk assessment. Environ Sci Pollut Res Int 24(1):874–885. https://doi.org/10.1007/s11356-016-7872-x

De Miguel E, Iribarren I, Chacón E, Ordoñez A, Charlesworth S (2007) Risk-based evaluation of the exposure of children to trace elements in playgrounds in Madrid (Spain). Chemosphere 66(3):505–513. https://doi.org/10.1016/j.chemosphere.2006.05.065

de Vicente I, Cruz-Pizarro L, Rueda FJ (2010) Sediment resuspension in two adjacent shallow coastal lakes: controlling factors and consequences on phosphate dynamics. Aquat Sci 72(1):21–31. https://doi.org/10.1007/s00027-009-0107-1

Ekino S, Susa M, Ninomiya T, Imamura K, Kitamura T (2007) Minamata disease revisited: an update on the acute and chronic manifestations of methyl mercury poisoning. J Neurol Sci 262(1–2):131–144. https://doi.org/10.1016/j.jns.2007.06.036

Gauze TKM, Kouassi KL, Malan DF (2019) Caracterisation de la dynamique d'occupation du sol et de la morphologie de la Lagune Aby Dans L'espace Du Parc National Des Îles Ehotile Sud-Est De La Cote d'Ivoire. Europ Sci J (**in French**). https://doi.org/10.19044/esj.2019.v15n2p11

Ghani SA, El Zokm G, Shobier A, Othman T, Shreadah M (2013) Metal pollution in surface sediment of Abu-Qir bay and Eastern harbour of Alexandria, Egypt. Egypt J Aquatic Res 39(1):1–12. https://doi.org/10.1016/j.ejar.2013.03.001

Ghosh SK, Lee J, Godwin AC, Oke A, Al-Rawin Elhoz M (2016) Waste management in USA through case studies: e-wastes recycling and waste to energy plant. J Solid Waste Tech Manag 42(1)

Hakanson L (1980) An ecological risk index for aquatic pollution control: a sedimentological approach. Water Res 14(8):975–1001. https://doi.org/10.1016/0043-1354(80)90143-8

Hamzeh M, Ouddane B, Daye M, Halwani J (2014) Trace metal mobilization from surficial sediments of the Seine River estuary. Water Air Soil Pollut 225(3):1878–1892. https://doi.org/10.1007/s11270-014-1878-0

Helali MA, Zaaboub N, Oueslati W, Added A, Aleya L (2016) Suspended particulate matter fluxes along with their associated metals, organic matter and carbonates in a coastal Mediterranean area affected by mining activities. Mar Pollut Bull 104(1–2):171–181. https://doi.org/10.1016/j.marpolbul.2016.01.041

Horowitz AJ, Elrick KA, Hooper RP (1989) The prediction of aquatic sediment-associated trace element concentrations using selected geochemical factors. Hydrol Process 3(4):347–364. https://doi.org/10.1002/hyp.3360030406

Hostache R, Hissler C, Matgen P, Guignard C, Bates P (2014) Modelling suspended-sediment propagation and related heavy metal contamination in floodplains: a parameter sensitivity analysis. Hydrol Earth Syst Sci 18(9):3539–3551. https://doi.org/10.5194/hess-18-3539-2014

Iqbal J, Tirmizi SA, Shah MH (2013) Statistical apportionment and risk assessment of selected metals in sediments from Rawal Lake (Pakistan). Environ Monit Assess 185(1):729–743. https://doi.org/10.1007/s10661-012-2588-y

Islam MS, Ahmed MK, Habibullah-Al-Mamun M, Hoque MF (2015) Preliminary assessment of heavy metal contamination in surface sediments from a river in Bangladesh. Environ Earth Sci 73(4):1837–1848. https://doi.org/10.1007/s12665-014-3538-5

Kim E, Little JC, Chiu N (2004) Estimating exposure to chemical contaminants in drinking water. Environ Sci Technol 38(6):1799–1806. https://doi.org/10.1021/es026300t

Kinimo KC, Yao KM, Marcotte S, KouassiTrokourey NLBA (2018) Preliminary data on arsenic and trace metals concentrations in wetlands around artisanal and industrial mining areas (Cote d'Ivoire, West Africa). Data Brief 18:1987–1994. https://doi.org/10.1016/j.dib.2018.04.105

Kouassi DNF, Yao KM, Coulibaly AS, Bi TJGI (2022) Trace metal concentrations, fluxes, and potential human health risks in West Africa Rivers: a case study on the Bia, Tanoé, and Comoé rivers (Cote D'Ivoire). Environ Monit Assess 194(7):475. https://doi.org/10.1007/s10661-022-09810-2

Li LJ, Zhang L, Wang H, Wang J, Yang JW, Jiang DJ, Li JY, Qin DY (2007) Assessing the impact of climate variability and human activities on streamflow from the Wuding River basin in China. Hydrol Process 21(25):3485–3491. https://doi.org/10.1002/hyp.6485

Loring DH, Rantala RT (1992) Manual for the geochemical analyses of marine sediments and suspended particulate matter. Earth-Sci Rev 32(4):235–283

Lü J, Jiao WB, Qiu HY, Chen B, Huang XX, Kang B (2018) Origin and spatial distribution of heavy metals and carcinogenic risk assessment in mining areas at You'xi County Southeast China.

Geoderma 310:99–106. https://doi.org/10.1016/j.geoderma.2017.09.016

Luo W, Lu YL, Wang TY, Hu WY, Jiao WT, Naile JE, Khim JS, Giesy JP (2010) Ecological risk assessment of arsenic and metals in sediments of coastal areas of northern Bohai and Yellow Seas, China. Ambio 39(5–6):367–375. https://doi.org/10.1007/s13280-010-0077-5

Maanan M, Saddik M, Maanan M, Chaibi M, Assobhei O, Zourarah B (2015) Environmental and ecological risk assessment of heavy metals in sediments of Nador lagoon, Morocco. Ecol Indic 48:616–626. https://doi.org/10.1016/j.ecolind.2014.09.034

Nyantakyi AJ, Akoto O, Fei-Baffoe B (2019) Seasonal variations in heavy metals in water and sediment samples from River Tano in the Bono, Bono East, and Ahafo Regions, Ghana. Environ Monit Assess 191(9):570. https://doi.org/10.1007/s10661-019-7744-1

Ouattara AA, Yao KM, Soro MP, Diaco T, Trokourey A (2018) Arsenic and trace metals in three West African Rivers: concentrations, partitioning, and distribution in particle-size fractions. Arch Environ Contam Toxicol 75(3):449–463. https://doi.org/10.1007/s00244-018-0543-9

Panagos P, Jiskra M, Borrelli P, Liakos L, Ballabio C (2021) Mercury in European topsoils: anthropogenic sources, stocks and fluxes. Environ Res 201:111556. https://doi.org/10.1016/j.envres.2021.111556

Ravichandran M, Baskaran M, Santschi PH, Bianchi TS (1995) History of trace metal pollution in Sabine-Neches estuary, Beaumont, Texas. Environ Sci Technol 29(6):1495–1503. https://doi.org/10.1021/es00006a010

Rumisha C, Elskens M, Leermakers M, Kochzius M (2012) Trace metal pollution and its influence on the community structure of soft bottom molluscs in intertidal areas of the Dar es Salaam coast, Tanzania. Mar Pollut Bull 64(3):521–531. https://doi.org/10.1016/j.marpolbul.2011.12.025

Samouhos M, Peppas A, Bartzas G, Taxiarchou M, Tsakiridis PE (2021) Arsenic release through refractory gold ore processing. Immobilization and decontamination approaches. Curr Opin Environ Sci Health 20:100236. https://doi.org/10.1016/j.coesh.2021.100236

Shil S, Singh UK (2019) Health risk assessment and spatial variations of dissolved heavy metals and metalloids in a tropical river basin system. Ecol Indic 106:105455. https://doi.org/10.1016/j.ecolind.2019.105455

Sinex SA, Helz GR (1981) Regional geochemistry of trace elements in Chesapeake Bay sediments. Environ Geol 3(6):315–323. https://doi.org/10.1007/BF02473521

Singh UK, Kumar B (2017) Pathways of heavy metals contamination and associated human health risk in Ajay River basin, India. Chemosphere 174:183–199. https://doi.org/10.1016/j.chemosphere.2017.01.103

Solgi E, Esmaili-Sari A, Riyahi-Bakhtiari A, Hadipour M (2012) Soil contamination of metals in the three industrial estates, Arak, Iran. Bull Environ Contam Toxicol 88(4):634–638. https://doi.org/10.1007/s00128-012-0553-7

Song JM, Liu QQ, Sheng YQ (2019) Distribution and risk assessment of trace metals in riverine surface sediments in gold mining area. Environ Monit Assess 191(3):191. https://doi.org/10.1007/s10661-019-7311-9

Taiwo AM, Awomeso JA (2017) Assessment of trace metal concentration and health risk of artisanal gold mining activities in Ijeshaland, Osun State Nigeria: part 1. J Geochem Explor 177:1–10. https://doi.org/10.1016/j.gexplo.2017.01.009

Turekian KK, Wedepohl KH (1961) Distribution of the elements in some major units of the Earth's crust. Geol Soc Am Bull 72(2):175. https://doi.org/10.1130/0016-7606(1961)72[175:DOTEIS]2.0.CO;2

USEPA (2004) Risk assessment guidance for Superfund, volume 1, human health evaluation manual (part E, Supplemental Guidance for Dermal Risk Assessment). Report EPA/540/R/99/005. US Environmental Protection Agency, Washington, DC

USEPA (2011) Regional Screening Level (RSL) Summary Table: November 2011. http://www.epa.gov/regshwmd/risk/human/Index.htm

US Environmental Protection Agency (EPA) (2012) Integrated Risk Information System of the US Environmental Protection Agency

Ustaoğlu F, Islam MS (2020) Potential toxic elements in sediment of some rivers at Giresun, northeast Turkey: a preliminary assessment for ecotoxicological status and health risk. Ecol Indic 113:106237. https://doi.org/10.1016/j.ecolind.2020.106237

Vallius H, Ryabchuk D, Kotilainen A (2007) Distribution of heavy metals and arsenic in soft surface sediments of the coastal area off Kotka, northeastern Gulf of Finland, Baltic Sea. In: Vallius H (ed.) Holocene sedimentary environment and sediment geochemistry of the Eastern Gulf of Finland, Baltic Sea', Special Paper, vol 45, pp 33–48

Wang YB, Liu CW, Wang SW (2015) Characterization of heavy-metal-contaminated sediment by using unsupervised multivariate techniques and health risk assessment. Ecotoxicol Environ Saf 113:469–476. https://doi.org/10.1016/j.ecoenv.2014.12.036

Xie WS, Peng C, Wang HT, Chen WP (2017) Health risk assessment of trace metals in various environmental media, crops and human hair from a mining affected area. Int J Environ Res Public Health 14(12):1595. https://doi.org/10.3390/ijerph14121595

Xu G, Pei SF, Liu J, Gao MS, Hu G, Kong XH (2015) Surface sediment properties and heavy metal pollution assessment in the near-shore area, north Shandong Peninsula. Mar Pollut Bull 95(1):395–401. https://doi.org/10.1016/j.marpolbul.2015.03.040

Zhang LP, Ye X, Feng H, Jing YH, Ouyang T, Yu XT, Liang RY, Gao CT, Chen WQ (2007) Heavy metal contamination in western Xiamen Bay sediments and its vicinity, China. Mar Pollut Bull 54(7):974–982. https://doi.org/10.1016/j.marpolbul.2007.02.010

Zhang ZX, Lu Y, Li HP, Tu Y, Liu BY, Yang ZG (2018) Assessment of heavy metal contamination, distribution and source identification in the sediments from the Zijiang River, China. Sci Total Environ 645:235–243. https://doi.org/10.1016/j.scitotenv.2018.07.026

Zhao SY, Zhu LX, Li DJ (2015) Microplastic in three urban estuaries, China. Environ Pollut 206:597–604. https://doi.org/10.1016/j.envpol.2015.08.027